 https://doi.org/10.3011/ESARDA.IJNSNP.2020.1

Performance of FRAM isotopic analysis of shielded plutonium with an electrically cooled coaxial gamma-spectrometer

Jozsef Zsigrai[1], Andrey Berlizov[2], Darcy van Eerten[1,3], Janos Bagi[1], Artur Muehleisen[1]

[1]European Commission, Joint Research Centre, Directorate G, Karlsruhe, Germany
[2]International Atomic Energy Agency, Vienna, Austria
[3]Durham University, Durham, United Kingdom

Abstract:

The capability of the FRAM software to accurately determine the isotopic composition of shielded plutonium was tested by the Joint Research Centre in Karlsruhe to support the use of FRAM for the verification of plutonium-bearing items by safeguards inspectors in the field. More than ten thousand spectra of eight certified reference-material items were analysed using different FRAM parameter sets. The spectra were recorded by the "ORTEC microDetective" portable electrically cooled coaxial gamma spectrometer. The performance of FRAM was evaluated as a function of shielding thickness, measurement time, sample composition and "spectrum quality". The spectrum quality was quantified using a numerical figure of merit that included the uncertainties of the peak areas relevant for the isotopic analysis. Thereby, it combined the effects of shielding, measurement time and sample isotopic composition into a single indicator. It was confirmed that using FRAM's automatic analysis option improves the isotopic results, especially in the case of lower quality spectra. The results of this work will help safeguards inspectors to optimize the use of electrically cooled gamma-spectrometers and to improve the accuracy of plutonium isotopic composition measurements in the field.

Keywords: gamma spectrometry, electrically cooled gamma spectrometer, plutonium isotopic composition, FRAM

1. Introduction

The purpose of this work was to study and possibly improve the capability of the FRAM software to determine the isotopic composition of shielded plutonium by portable electrically cooled HPGe detectors. This work, focused on plutonium, is a follow-up of previous work [1] that was focused on uranium. Both tasks were carried out within the European Commission's support programme to the International Atomic Energy Agency (IAEA). For the sake of completeness, some introductory remarks about the task and about FRAM are repeated here.

FRAM is software that calculates uranium and plutonium isotopic composition from the gamma spectra of these materials [2], [3]. It has been developed at Los Alamos National Laboratory (USA) and it has been commercialized by ORTEC and Canberra. The version used in this study was 5.2, which has minor changes compared to version 5.1 [4], which was used in the study on uranium [1].

The so-called parameter sets determine what FRAM exactly does. They define the type of material (U, Pu, MOX) and the type of detector. They also contain information about the isotopes and gamma peaks to be analysed, peak fitting parameters, energy calibration, relative efficiency constraints, etc. FRAM contains a number of default parameter sets built into the software, which cover a large number of typical measurement configurations. However, users can also prepare modified or new parameter sets to suit their specific measurement configuration. In this work we focused on parameter sets for plutonium.

More than 7000 high-resolution gamma spectra of various certified reference materials were taken by the ORTEC microDetective electrically cooled spectrometer under well-defined measurement conditions with different steel, cadmium and lead screens. These spectra were used to check the performance of FRAM v5.2 for determining the isotopic composition of shielded plutonium. In this paper the results calculated using different parameter sets are compared to each other and the influence of shielding thickness, measurement time and plutonium burn-up is discussed. This way the capabilities and limitations of FRAM became better understood.

2. Method and equipment

The ORTEC microDetective electrically cooled spectrometer [5] was used to record the gamma spectra. It has a high-purity coaxial germanium (HPGe) crystal of 50 mm diameter and 30 mm depth (length). The conversion gain of its amplifier was set to 0.125 keV/channel, to match the gain in the default FRAM parameter sets. The amplifier rise time was set to 3.4 μs, and flattop to 0.8 μs. (Note that for the uranium study [1] an older version of the ORTEC detective was used, having fixed settings, set in the factory.) The measured peak resolution (full with at half-maximum) was approximately 1.5 keV at 122 keV and 2.0 keV at 1001 keV.

A total of 8 Pu reference items from the "CBNM" [6] and "PIDIE" [7], [8], [9] sets were used in this study. Their isotopic

Zsigrai, J., Berlizov, A., van Eerten, D., Bagi, J., & Muehleisen, A. (2020). Performance of FRAM isotopic analysis of shielded plutonium with an electrically cooled coaxial gamma-spectrometer. *ESARDA Bulletin - The International Journal of Nuclear Safeguards and Non-proliferation*, 60, 2-19. https://doi.org/10.3011/ESARDA.IJNSNP.2020.1

Reference sample		Isotope					
		^{238}Pu	^{239}Pu	^{240}Pu	^{241}Pu	^{242}Pu	^{241}Am
CBNM Pu93	weight %	0.0117	93.4123	6.3131	0.2235	0.0395	0.1047
	2s	0.00003	0.004	0.0039	0.0004	0.0003	0.0021
CBNM Pu84	weight %	0.0703	84.3377	14.2069	1.0275	0.3576	0.2173
	2s	0.0006	0.0084	0.0085	0.0018	0.001	0.0022
CBNM Pu70	weight %	0.8458	73.3191	18.2945	5.4634	2.0772	1.1705
	2s	0.0018	0.0098	0.0087	0.0034	0.0023	0.0117
CBNM Pu61	weight %	1.1969	62.5255	25.4058	6.6793	4.1925	1.4452
	2s	0.0025	0.0283	0.0241	0.0087	0.0064	0.0144

Table 1: Isotopic composition of the "CBNM" reference samples in weight % with 2s absolute uncertainty for reference date 20.6.1986.

Reference sample		Isotope					
		^{238}Pu	^{239}Pu	^{240}Pu	^{241}Pu	^{242}Pu	^{241}Am
PIDIE 1	weight %	0.01101	93.7650	5.99025	0.19920	0.0346	0.2304
	2s	0.00033	0.0065	0.0052	0.00255	0.0015	0.0060
PIDIE 3	weight %	0.04716	84.5795	14.1442	0.9953	0.2338	0.6282
	2s	0.00038	0.0094	0.0052	0.0036	0.0075	0.0151
PIDIE 5	weight %	0.1314	75.8862	21.2169	2.0638	0.7017	1.7488
	2s	0.0011	0.0147	0.0115	0.0042	0.0015	0.0387
PIDIE 7	weight %	1.253	61.9848	25.5941	6.4919	4.6763	3.5287
	2s	0.016	0.0420	0.0195	0.0132	0.0081	0.1111

Table 2: Isotopic composition of PIDIE reference samples in weight % (normalized to sum of Pu isotopes) with 2s absolute uncertainty for reference date 1.1.1988.

composition is shown in Table 1 and Table 2. The CBNM set consists of four sintered plutonium oxide pellets encased in stainless steel and protected by a plastic cap. Each pellet in the CBNM set contains 6.65±0.06 g of PuO_2. The items in the PIDIE set contain ca. 0.425g Pu in the form of a pressed PuO_2 pellet in a welded steel container.

The spectra of each item were recorded using a tungsten collimator and combinations of Fe screens of up to 16 mm thickness, Cd screens up to 2 mm thickness and a Pb screen of 4 mm thickness. This means 5 shielding configurations for each sample (Table 3). The sample to detector distance was 10 cm. There were two exceptions measured at 20 cm. These were the configurations with the CBNM Pu61 source and low shielding (2 mm Cd with no Fe and 1 mm Cd with 4 mm Fe). These two configurations could not be measured at 10cm because the count rate was too high and it saturated the spectrometer.

CBNM				PIDIE			
Fe	Cd	Pb	Effective Fe	Fe	Cd	Pb	Effective Fe
0	2	0	4	0	1.5	0	3
4	1	0	6	4	0.5	0	5
8	0.5	0	9	8	0	0	8
16	0	0	16	16	0	0	16
0	0	4	27	0	0	4	27

Table 3: Shielding thicknesses in mm. ("Effective Fe" is defined below.)

In Figure 1 the dependence of the dead time on the effective iron shielding thickness is shown for each sample. The total count rate ranged from about 200 cps (e.g. for PIDIE1 with 4 mm Pb) to about 6000 (e.g. for CBNM 61 with 2 mm Cd).

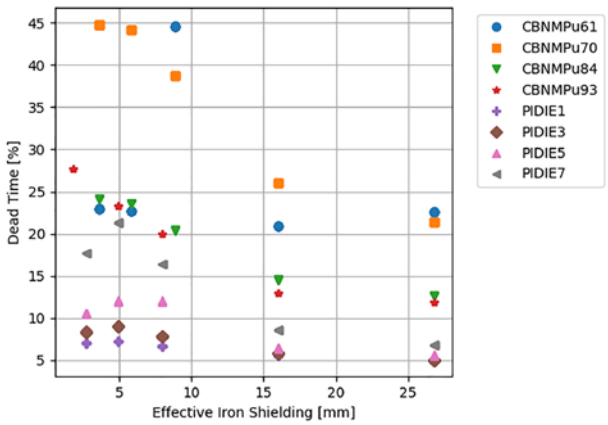

Figure 1: Dead time as a function of effective iron shielding. The two first points for CBNMPu61 have lower dead time than the third point in this series, because they were measured at a 20 cm distance, instead of 10 cm, to avoid saturating the detector.

In each of the 5 shielding configurations, for each sample 192 spectra of 5 minutes real time were recorded (that is 5x8x192=7680 spectra). Sum spectra of 15 minutes, 90 minutes, 2 hours, 4 hours, 6 hours and 16 hours real

time were prepared from the 5-minute spectra. This gives a total of 11240 spectra, distributed into 7 sets according to their real time.

The spectra within each set are independent from each other. The sets are not independent from each other, because each set was prepared from the same base set of 5-minute spectra. Therefore, comparing FRAM results obtained with different sets shows the dependence of the results on the measurement time, without interference of other factors.

All spectra were analysed with 3 parameter sets, with and without the “autoanalysis” option:

- Pu_Cx_120-460, no autoanalysis
- Pu_Cx_180-1010, no autoanalysis
- Pu_Cx_120-460, with autoanalysis
- Pu_Cx_180-1010, with autoanalysis
- det_coax_120_800_1_ecgs, no autoanalysis

The parameter sets Pu_Cx_120-460 and Pu_Cx_180-1010 are defaults in FRAM v5.2, while det_coax_120_800_1_ecgs was provided to us by the IAEA. For the parameter set det_coax_120_800_1_ecgs the auto analysis option is not applicable. The numbers in the names of the parameter sets indicate the energy range in keV used in the analysis. With the auto analysis option the analysis is repeated with another parameter set if during the first analysis certain criteria are met (e.g. ratio of selected peaks). This makes it possible, for example, to automatically reanalyse spectra of shielded samples with a parameter set that uses the higher energy range.

Scripts written in the Python 3.6 programming language were used for

- adding the spectra,
- running FRAM on 11240 spectra with different parameter sets,
- extracting the results of interest from the FRAM result files,
- calculating performance indicators, such as relative bias, "MARD" and "CBD", defined below,
- visualizing the performance of FRAM through the use of various graphs. The FRAM results plotter received a graphical user interface shown in Figure 2.

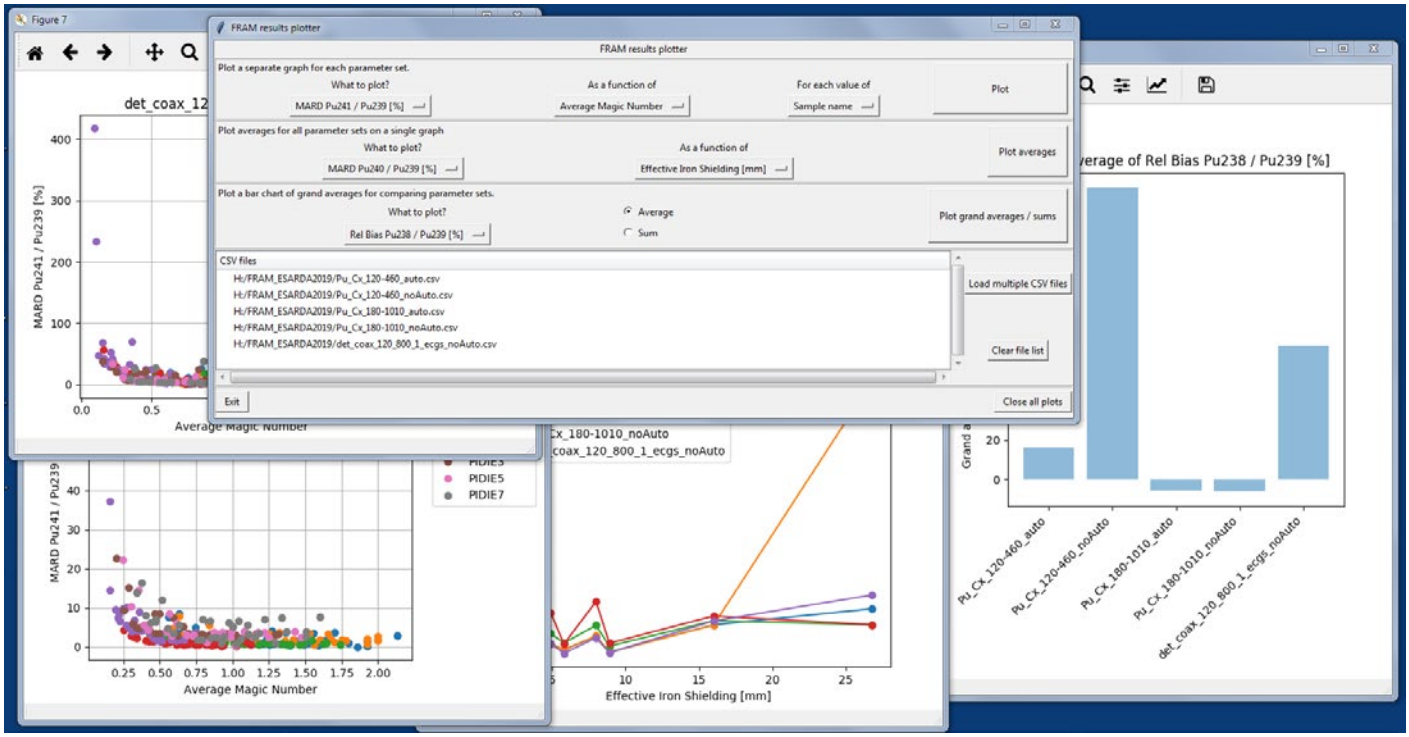

Figure 2: Screenshot of the FRAM results plotter

Several quantities were calculated for the statistical interpretation of the results.

- Average relative bias (ARB):
  - The systematic component of FRAM's bias, or the expected accuracy of many (*n*) measurements. It can be either positive or negative.
- Relative standard deviation (RSD):
  - The random component of FRAM's bias.
- Combined average relative bias and relative standard deviation (CBD):
  - The overall performance of FRAM, or the expected accuracy of a single measurement.
- Mean absolute value of the relative difference (MARD):
  - Similar to, but different from CBD. It also describes overall performance of FRAM, or the expected accuracy of a single measurement, but using it in error propagation is not straightforward. Here it is only used for comparison with previous work on uranium [1].

All these quantities are calculated for each sample, for each shielding configuration for each measurement time. They are defined as follows:

$$Average\ Relative\ Bias = ARB = \frac{\sum_{i=1}^{n} \frac{x_i - x_{Ref}}{x_{Ref}}}{n},$$

$$Relative\ Standard\ Deviation =$$

$$= RSD = \frac{1}{x_{Avg}} \sqrt{\frac{\sum_{i=1}^{n} \left(x_i - x_{Avg}\right)^2}{n-1}},$$

$$Combined\ Bias\ and\ standard\ Deviation =$$

$$= CBD = \sqrt{ARB^2 + RSD^2},$$

$$Mean\ Absolute\ value\ of\ Relative$$

$$Difference = MARD = \frac{\sum_{i=1}^{n} \frac{\left|x_i - x_{Ref}\right|}{x_{Ref}}}{n}, \quad (1)$$

where n is the number of spectra analysed (e.g. n=192 for the 5-minute spectra), x_i is the value calculated by FRAM, x_{Ref} is the certified reference value and x_{Avg} is the average of the FRAM results for the given measurement time and shielding configuration. For the 16 h spectra n=1, so RSD is not calculated for the 16 h spectra.

In this work all isotopic data (declared data and FRAM results) were decay-corrected to 1st January 2019 and all quantities were calculated for this reference date.

Two especially important variables used for plotting were the effective iron shielding and the statistical quality indicator of the spectra. The effective iron shielding is the equivalent shielding based on thickness of the shielding screens used and the mean values of the linear attenuation coefficients in the energy range 180-433 keV. It is calculated as:

$$Effective\ iron\ shielding = d_{Fe} + \frac{\bar{\mu}_{Cd}}{\bar{\mu}_{Fe}} d_{Cd} + + \frac{\bar{\mu}_{Pb}}{\bar{\mu}_{Fe}} d_{Pb}, \quad (2)$$

where d_X, is the thickness of the Fe, Cd or Pb screens used and $\bar{\alpha}_X$ is the average of 14 equidistant values of the linear attenuation coefficient of these materials in the energy range 180-433 keV. The values for linear attenuation coefficients were taken from the online NIST database [10].

For example, 4 mm of Pb corresponds to 26.8 mm effective iron shielding, while 2 mm of Cd corresponds to 3.6 mm effective iron shielding, according to the above definition.

The indicator of the statistical quality of the spectra ("magic number") is the inverse of the combined relative uncertainty of the "magic peaks":

$$statistical\ indicator\ \left("magic\ number"\right) = \frac{1}{\sqrt{\sum_i \delta_i^2}}, \quad (3)$$

where δ_i is the relative uncertainty of the i^{th} peak and the sum goes over all magic peaks. The "magic peaks" are those peaks which are used in all parameter sets investigated in this study. In particular, they were the peaks of ^{239}Pu, ^{241}Pu and ^{241}Am at 413.712, 208.000 and 335.432 keV, respectively.

The statistical indicator depends on the following:

- measurement time,
- shielding,
- sample activity
- and isotopic composition.

Figure 3 shows the dependence of the statistical indicator (averaged over all shieldings and samples) on the measurement time, for all investigated parameter sets.

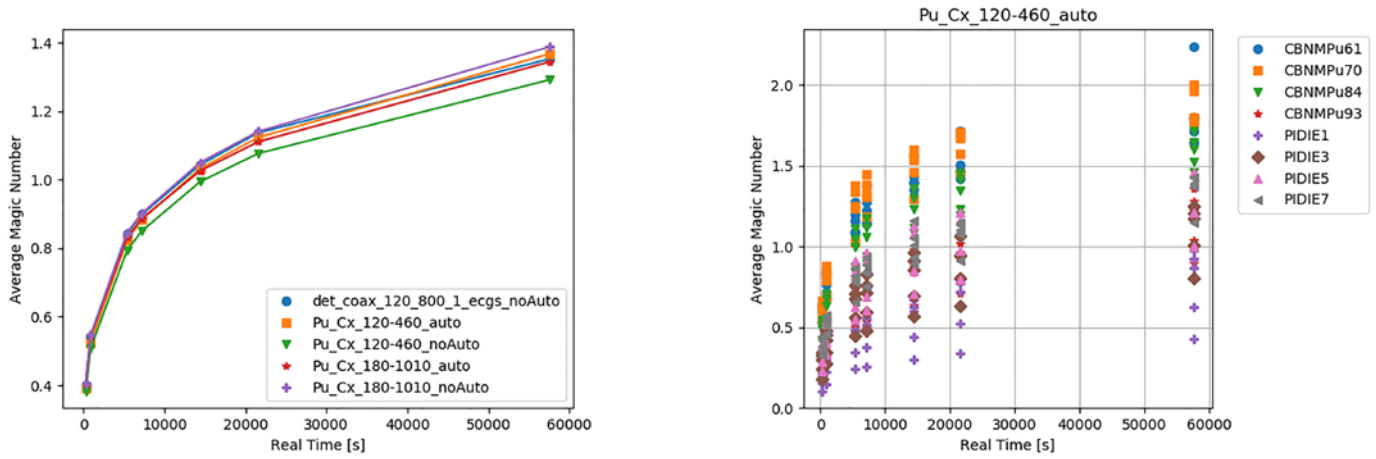

Figure 3: Left: statistical quality of the spectra ("magic number") averaged over all shieldings and samples as a function of real measurement time, for all investigated parameter sets. Right: statistical quality of the spectra ("magic number") as a function of real measurement time for all samples calculated using the parameter set Pu_Cx_120-460 with auto analysis turned on.

The statistical indicator also slightly depends on the parameter set, due to small differences in peak fitting. It increases with measurement time, but for some samples (e.g. PIDIE1, which has low activity) its stays quite low even for long measurement times, especially in the case of thick shielding. As it will be seen later, "good" spectrum quality means that the value of this indicator is around 1 or above 1. Note that, although the isotopic composition of, e.g., CBNMPu61 and PIDIE7 is very similar, their activity is very different. Therefore, their statistical indicators are very different.

Three different types of plots were prepared from the calculated statistical quantitates:

1. *"Category plots":* The performance indicators (average relative bias, RSD, CBD and MARD) of the isotope ratios relative to ^{239}Pu and of the ^{239}Pu isotope fraction were calculated for each configuration, each measurement time, each sample and each parameter set. These values were plotted as a function of various variables for all values of a selected category on a separate graph for each parameter set. For example, the dependence of ^{239}Pu CBD on spectrum quality for each value of the declared ^{239}Pu fraction is plotted on a separate graph for a given parameter set (Figure 14). This gives (5 configurations) x (7 different measurement times) x (8 samples) = 280 points on each "category plot".
2. "*Average plots*": To visualize FRAM's performance in a more compact form, the average of the above quantities was calculated as a function of selected variables and all parameter sets were plotted on the same graph. For example, the ^{239}Pu average CBD as a function of statistical quality of the spectra (Figure 13) plotted on the same graph for all parameter sets. In this case the number of points on the graph depends on the number of different values that the independent parameter may take.
3. "*Grand average plots" (bar charts)*": To have an even more compact comparison of the parameter sets, the grand averages of all the values of selected quantities calculated by a given parameter set were plotted on a bar chart. An example is the bar chart showing the grand average of the ^{241}Pu CBD for all parameter sets (Figure 6).

These plots demonstrate the performance of the different FRAM parameter sets for different situations and might be used for improving the parameter sets.

3. Results

3.1 General comments on the results

The presentation of the results starts by comparing the parameter sets using the grand average plots for each investigated quantity, and then goes into more detail using the average plots. There is no separate section for category plots, but category plots are present in Figure 14 and Figure 16, to better illustrate some conclusions from the average plots.

The results for ^{242}Pu were not investigated in this work, because ^{242}Pu cannot be directly obtained from the gamma spectrum and empirical correlations have to be used. The discussion of these empirical correlations will be the subject of further work. That is why only isotope ratios to ^{239}Pu are studied in this work, and not the ratios to total Pu, because the ratios to total Pu are affected by the calculation of ^{242}Pu. Nevertheless, due to its importance for safeguards, the ratio of ^{239}Pu to total Pu is also presented in this work. The ^{239}Pu results obtained in two different ways are shown: using the default ^{242}Pu correlation in the FRAM parameter set, and also by using the declared ^{242}Pu content.

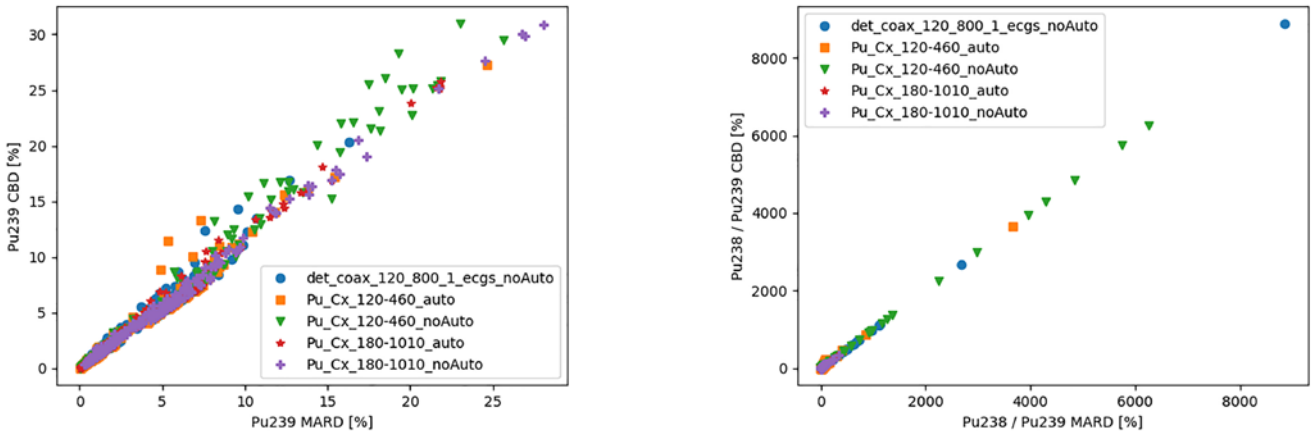

Figure 4: The CBD as a function of MARD for ^{239}Pu (left) and for the ^{238}Pu/^{239}Pu ratio right, for all investigates parameter sets.

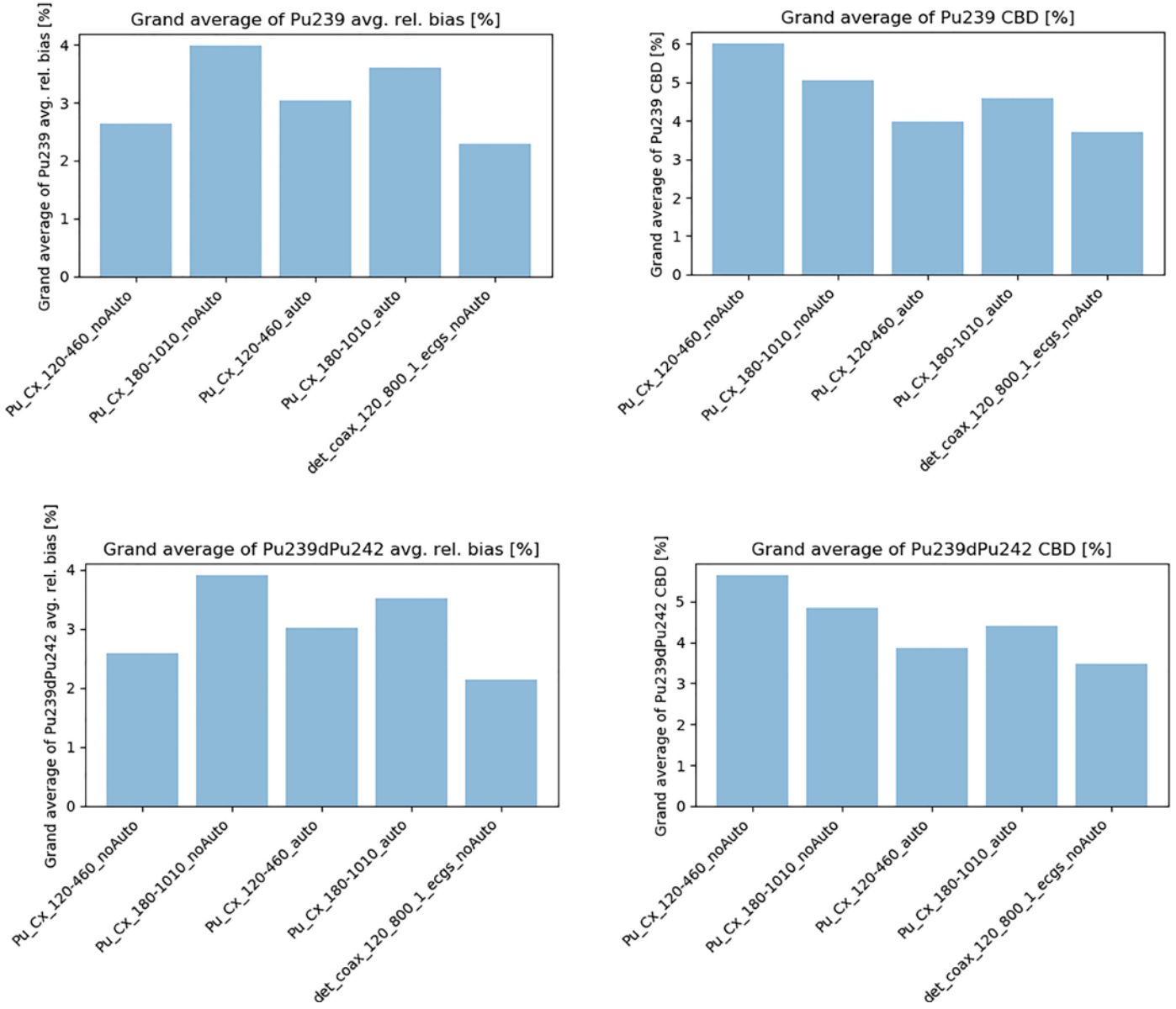

Figure 5: The grand average of ^{239}Pu/Pu mass fraction relative bias and CBD for all parameter sets, The upper plots show the results using the algorithm for ^{242}Pu calculation built in into the parameter sets, while the lower plots show the results using the (decay-corrected) declared ^{242}Pu.

In certain situations FRAM reports zero for some isotope ratios. Those results are removed from the averages presented in the graphs.

As the MARD used in previous work is no longer used here for the presentation of the results, it is worth to compare it to the CBD, which is used instead of it. The MARD and the CBD are mathematically NOT equivalent, but if all the biases are positive, then for large *n* (number of spectra) the values of the MARD and CBD are very close to each other. This is demonstrated in Figure 4, where the CBD for ^{239}Pu and for the ^{238}Pu/^{239}Pu ratio are plotted as a function of MARD.

3.2 Overall FRAM performance

To investigate overall FRAM performance, the grand average plots are best suited. They are supplemented with some average plots to explain in more detail the conclusions drawn from the grand average plots.

For the ^{239}Pu fraction the lowest grand average bias and the lowest grand average CBD are achieved using the parameter set det_coax_120_800_1_ecgs (Figure 5). This is true regardless of whether the built-in ^{242}Pu correlation or the declared ^{242}Pu values are used in the calculation. For mass ratios the best results are achieved with the two default parameter sets used in “autoanalysis” mode, and not with the det_coax_120_800_1_ecgs (Figure 6). These two observations seem to contradict each other. To resolve this seeming contradiction one has to notice two things:

- The ^{239}Pu biases with the parameter set det_coax_120_800_1_ecgs are both positive and negative, while with the default parameter sets they are mostly positive (except a few points) as seen on Figure 7. This way the individual ^{239}Pu biases for det_coax_120_800_1_ecgs cancel out, while for the other parameter set they do not, so the grand average is the lowest for det_coax_120_800_1_ecgs.
- From Figure 7 one can also see that the ^{239}Pu bias is correlated to the ^{240}Pu/^{239}Pu bias. For other mass ratios there is no such evident correlation. This is understandable, as ^{240}Pu is the second most abundant isotope after ^{239}Pu in all samples. This means that parameter sets which have lower absolute bias for ^{240}Pu/^{239}Pu will also have lower bias for ^{239}Pu. The correlation between the ^{239}Pu bias and ^{240}Pu/^{239}Pu bias is not linear: even a small negative bias of ^{240}Pu/^{239}Pu leads to a high ^{239}Pu bias, while relatively large positive ^{240}Pu/^{239}Pu biases lead to relatively low ^{239}Pu biases. For the parameter set det_coax_120_800_1_ecgs the ^{240}Pu/^{239}Pu biases are mostly positive, leading to small ^{239}Pu bias.

Therefore, the above points explain why from all investigated parameter sets the set det_coax_120_800_1_ecgs gives the lowest bias for the ^{239}Pu fraction, despite not giving the best results for the isotope ratios.

The above points also show that, to improve the results for ^{239}Pu, one should concentrate on improving the results for ^{240}Pu/^{239}Pu.

The grand average relative bias and CBD of the mass ratios relative to ^{239}Pu are shown for all parameter sets in Figure 6.

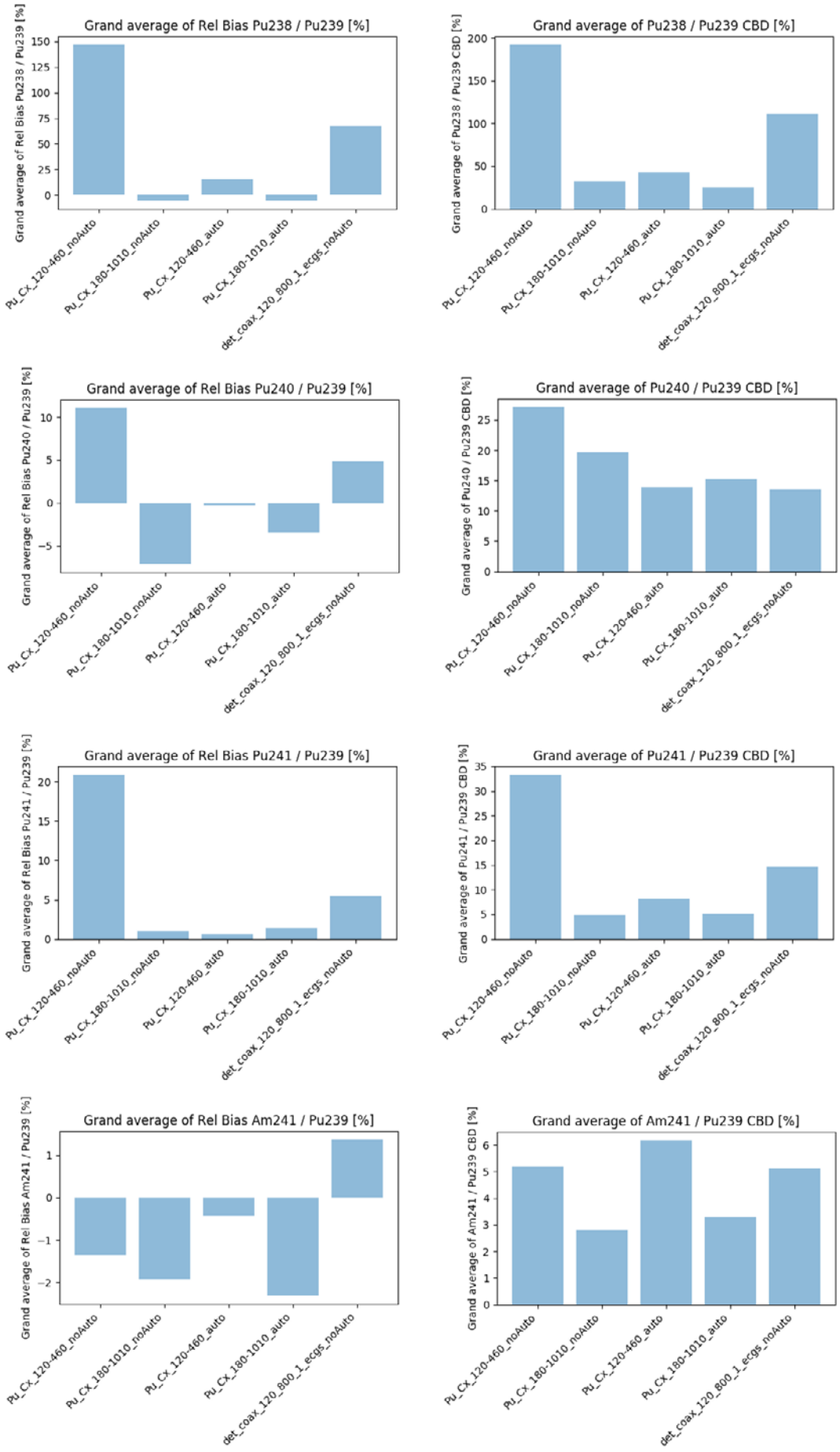

Figure 6: The grand average of the relative bias and CBD of the mass ratios for all parameter sets

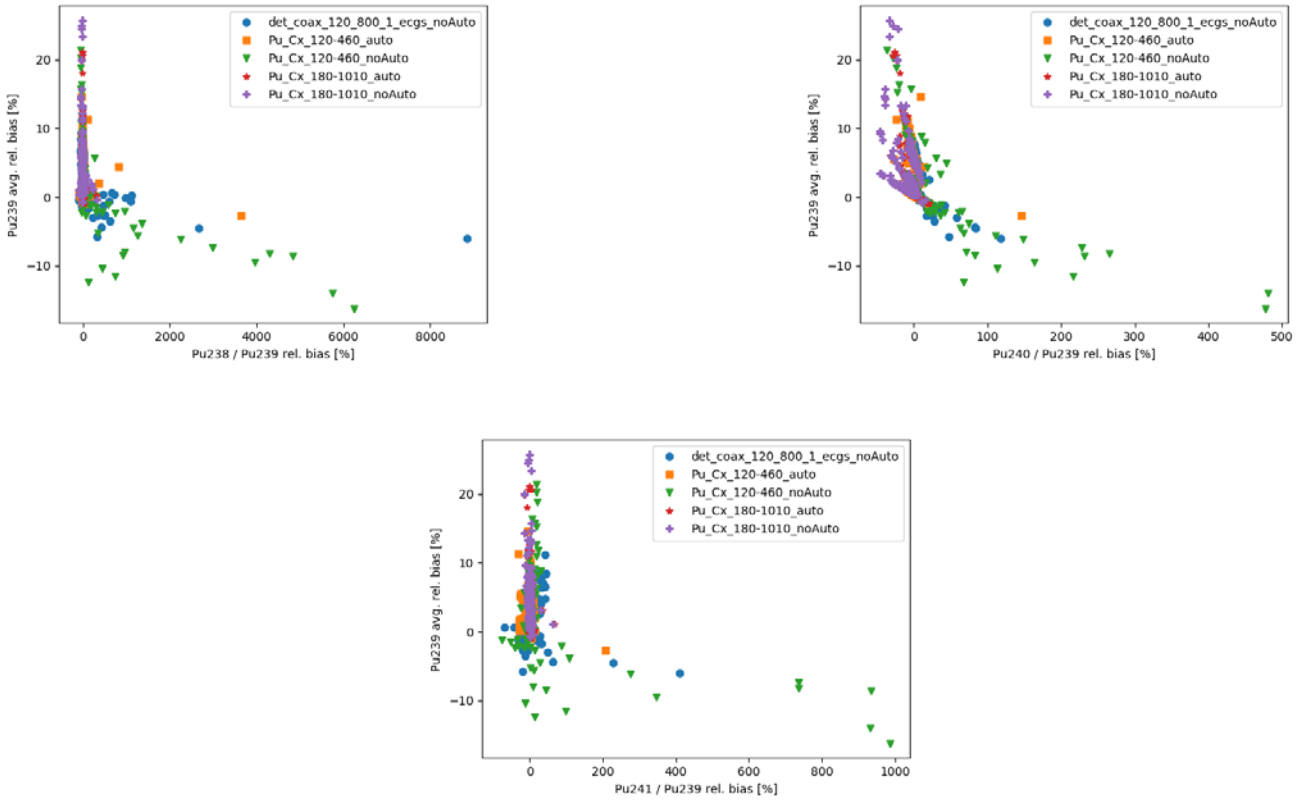

Figure 7: The average relative bias of the ^{239}Pu fraction as a function of the bias of the individual mass ratios, calculated using the ^{242}Pu correlation built in into the parameter sets. The plots calculated using the declared ^{232}Pu value are very similar.

3.3 FRAM performance in more detail

The “average plots” show the dependence of a selected quantity as a function of a measurement parameter, averaged over all identical values of that parameter in all spectra for which the selected parameter has the same value. For example, one of the points on an average plot can be the average of all spectra for which the effective shielding thickness is 16 mm, for all measurement times, for a given parameter set. The average depends on the grouping: e.g. grouping according to shielding, grouping according to spectrum quality, or grouping according to any other quantity. The parameters (groupings) investigated here are the shielding thickness and spectrum statistical quality.

3.3.1 Dependence of FRAM performance on spectrum statistical quality

The dependence of the CBD of the mass ratios on spectrum quality is shown in Figure 8. The relationship between FRAM’s reported uncertainty and spectrum quality is demonstrated in Figure 9 to Figure 12. The CBD of ^{239}Pu/Pu mass fraction is shown in Figure 13 and Figure 14.

The measurement uncertainty is related to the spectrum quality. The counting uncertainties reported by FRAM for the mass ratios are shown in Figure 9 as a function of spectrum statistical quality. To illustrate how the CBD and RSD are related to the counting uncertainty Figure 10 to Figure 12 show the RSD, CBD and average bias for the ^{240}Pu/Pu mass ratio, as a function of the reported counting uncertainty. These figures confirm that the counting uncertainty reported by FRAM mostly covers the calculated RSD, as long as one considers “reasonable” measurements, with good spectrum quality leading to uncertainties below approximately 60%. The CBD is slightly higher than the reported counting uncertainty, due to the bias of the results. The bias can be accounted for in the FRAM parameter sets by adding a constant systematic uncertainty term. Unfortunately, the bias is not constant and depends on the measurement uncertainty (that is, on spectrum quality), as illustrated in Figure 11.

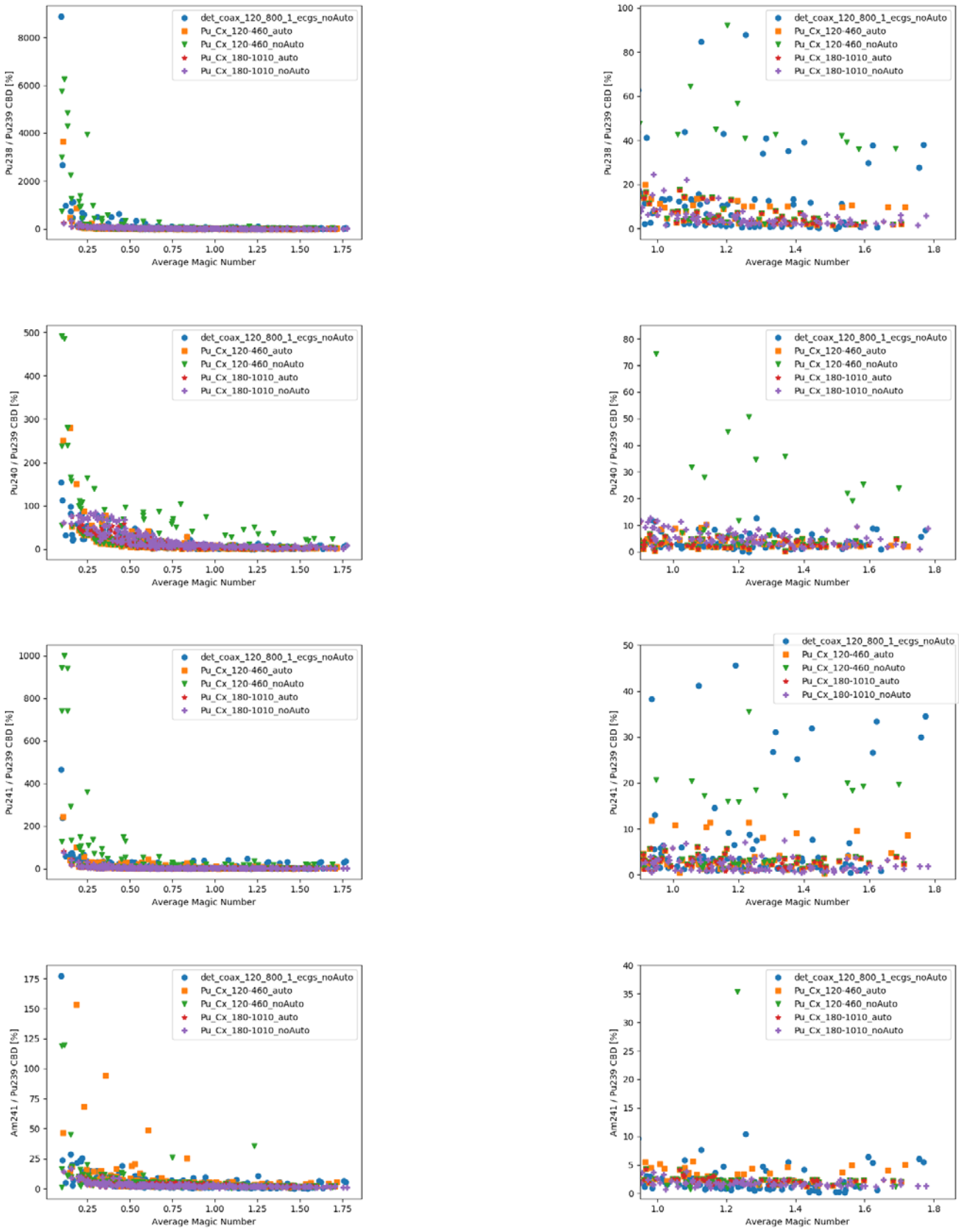

Figure 8: Average-plots of the CBD of the mass ratios as a function of statistical quality of the spectra. Left: entire range. Right: zoomed-in to higher spectrum quality.

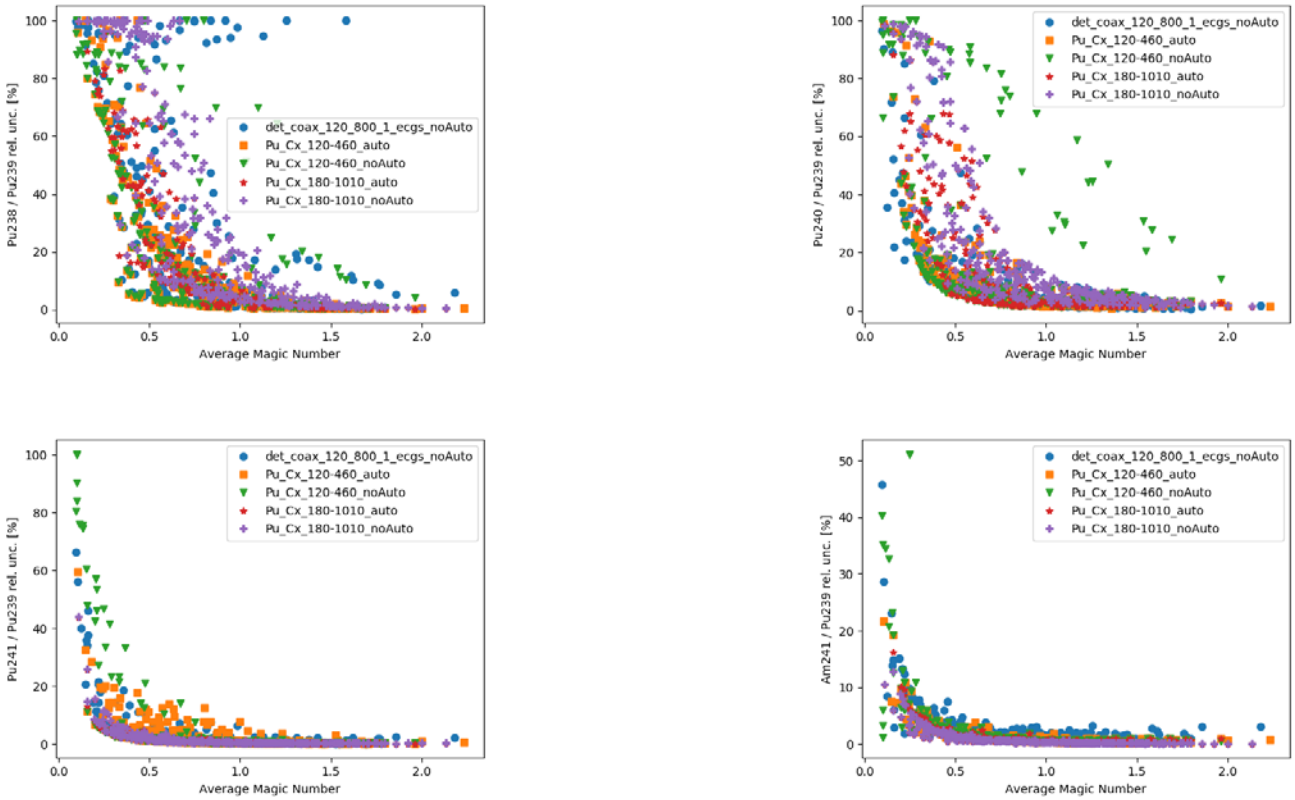

Figure 9: Average uncertainty of the mass ratios reported by FRAM, as a function of spectrum statistical quality

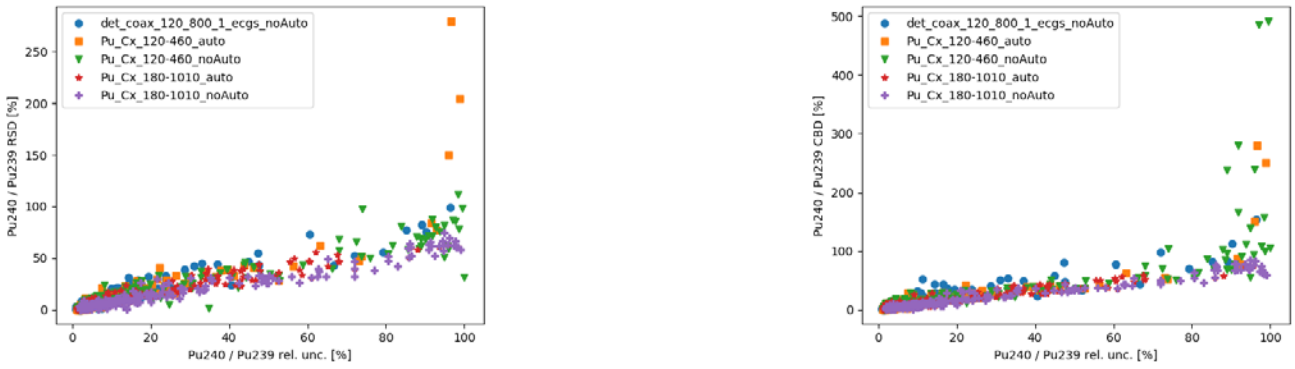

Figure 10: RSD and CBD of the ^{240}Pu/Pu ratio as a function of the reported counting uncertainty

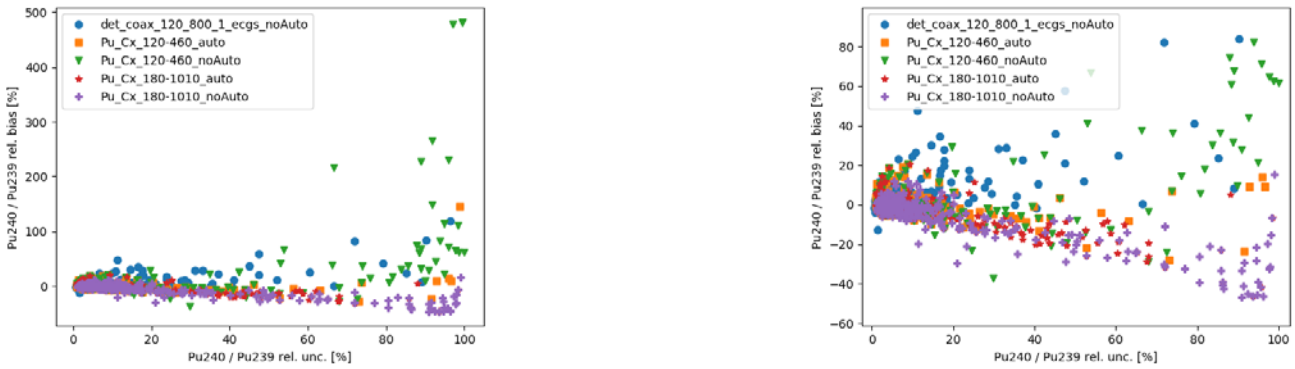

Figure 11: Average relative bias of the ^{240}Pu/Pu ratio as a function of the reported counting uncertainty. Left: entire plot. Right: zoomed-in to lower biases.

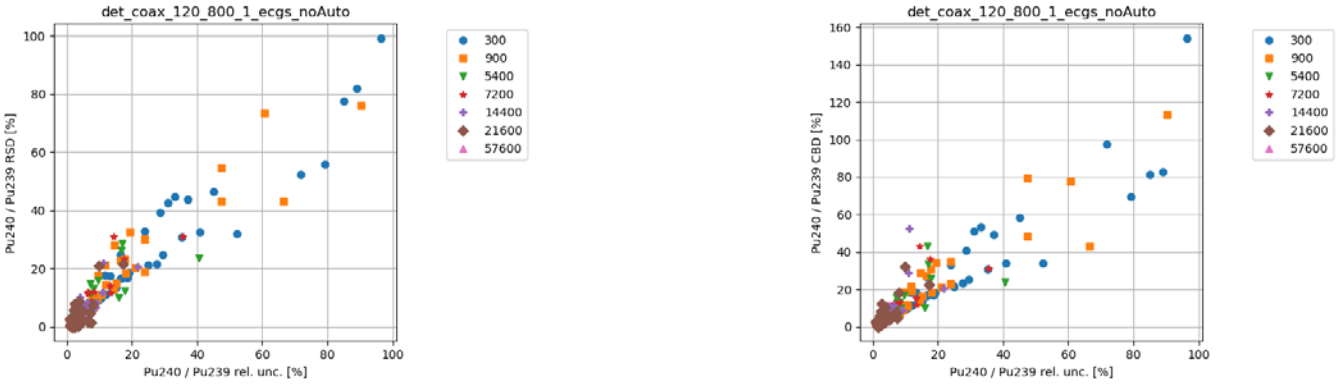

Figure 12: RSD and CBD of the ^{240}Pu/Pu ratio calculated using the parameter set det_coax_120_800_1_ecgs_noAuto, as a function of the reported counting uncertainty, for each value of the real time

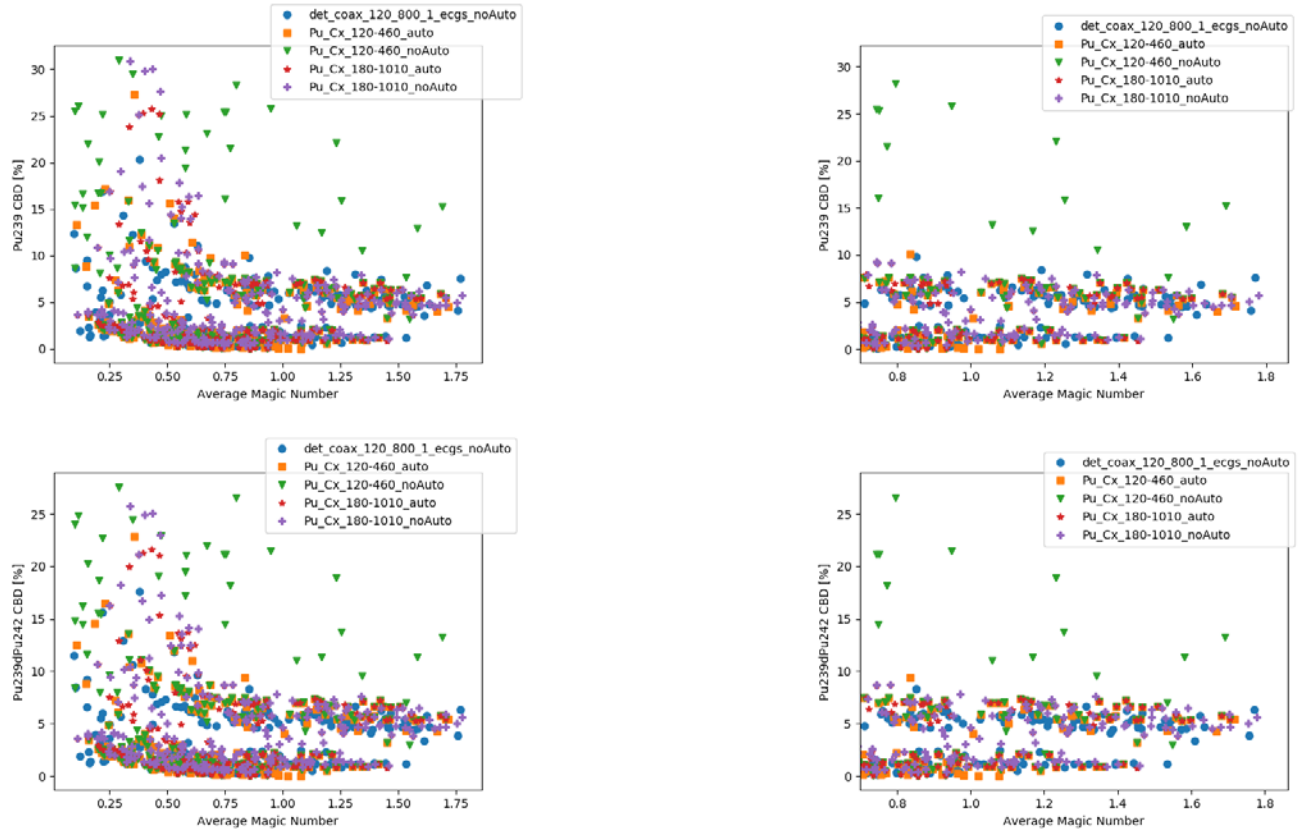

Figure 13: Average plot of the CBD of ^{239}Pu fraction as a function of statistical quality of the spectra: entire range (left) and zoomed-in to higher spectrum quality (right). The upper plots show the results using the algorithm for ^{242}Pu calculation built in into the parameter sets, while the lower plots show the results using the (decay-corrected) declared ^{242}Pu.

The average plots of the CBD of the mass ratios relative to ^{239}Pu as a function of statistical quality of the spectra show that all parameter sets give very bad results for low spectrum quality (meaning short measurement time and/or low sample activity and/or thick shielding). If the statistical indicator is above 1, then for most parameter sets the average CBD of ^{238}Pu/^{239}Pu becomes lower than 20%, the CBD of ^{240}Pu/^{239}Pu lower than 15%, the CBD of ^{241}Pu/^{239}Pu lower than 10 % and the CBD of ^{241}Am/^{239}Pu lower than 5 %. The CBD for Pu_Cx_120-460_noAuto and sometimes for det_coax_120_800_1_ecgs_noAuto is relatively high even for good spectrum quality. The reason is that these two parameter sets make use of the lower energy lines, which for shielded samples have high uncertainties even if the overall spectrum quality is relatively good.

The CBD of the ^{239}Pu/Pu fraction for good quality spectra is lower than 10 % for most parameter sets. However, Figure 13 shows two distinct groups of points: the points denoting higher CBD belong to high-burnup Pu (lower ^{239}Pu fraction), while the lower CBD belongs to low-burnup Pu. This is confirmed by Figure 14, showing the dependence of ^{239}Pu CBD on spectrum quality for each value of the declared ^{239}Pu fraction (a “category plot”) for the parameter set det_coax_120_800_1_ecgs.

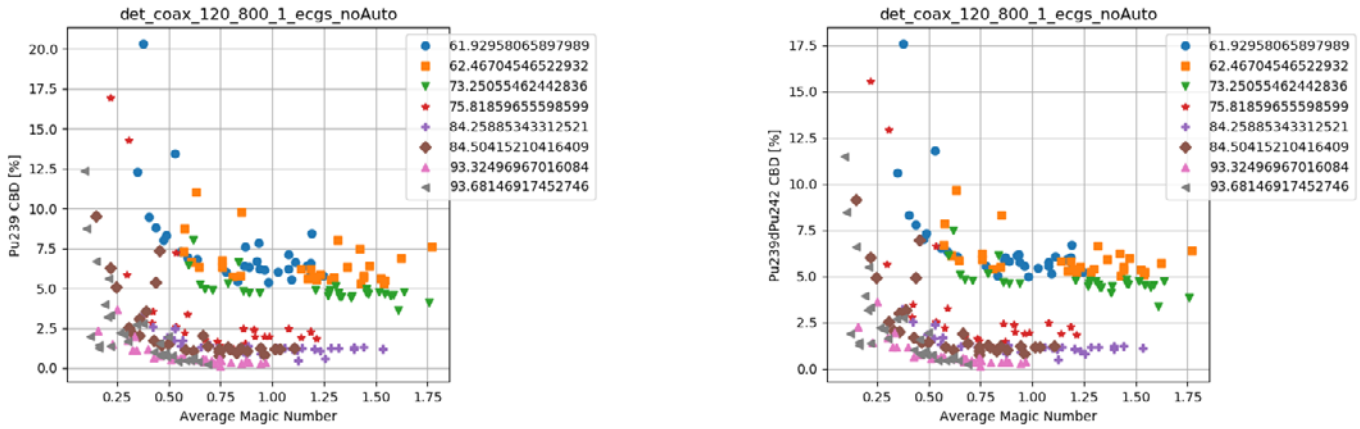

Figure 14: Dependence of ^{239}Pu CBD on spectrum quality for each value of the declared ^{239}Pu fraction (a "category plot") for the parameter set det_coax_120_800_1_ecgs. The left plot shows the results using the algorithm for ^{242}Pu calculation built in into the parameter sets, while the right plot shows the results using the (decay-corrected) declared ^{242}Pu.

3.3.2 Dependence of FRAM performance on shielding

The best results for the mass ratios are mostly obtained between 4-10 mm of effective iron (Figure 15). For effective iron shielding of 27 mm (i.e. a 4 mm sheet of Pb), the mass ratios calculated by the parameter sets that rely on lower energy peaks are biased by a few orders of magnitude, because in this case the low energy peaks cannot be reasonably analysed.

Contrary to the mass ratios, the results for the ^{239}Pu fraction are the best for the lowest shielding thickness (Figure 16). For all other shielding thicknesses the ^{239}Pu results are biased between about 2 and 5 % for all parameter sets. The ^{239}Pu fraction is calculated from the mass ratios, so why are the ^{239}Pu results best for the lowest shielding, when for the mass ratios the best results are obtained between 4-10 mm shielding? This is explained in the next paragraph.

Notice that ^{240}Pu/Pu, which has the strongest influence on ^{239}Pu, has a small positive bias for the lowest shielding. As discussed in section 3.2 about grand average plots, a positive bias in ^{240}Pu/Pu leads to a small bias in ^{239}Pu, while a negative bias in ^{240}Pu/Pu leads to a large ^{239}Pu bias. Therefore, out of the available results, the best ^{239}Pu results are those for which ^{240}Pu/Pu has a small positive bias.

In Figure 16 there are two distinct sets of points for each parameter set, just like in Figure 13 and Figure 14. The explanation for having these two groups is given by the "category plot" on the right of Figure 16 showing the ^{239}Pu relative bias as a function of effective iron shielding, for all values of the declared ^{239}Pu for the parameter set Pu_Cx_180-1010 with auto analysis turned on. On the right we see that the points with higher burnup (lower ^{239}Pu) have higher bias, resulting in the distinct groups on the left.

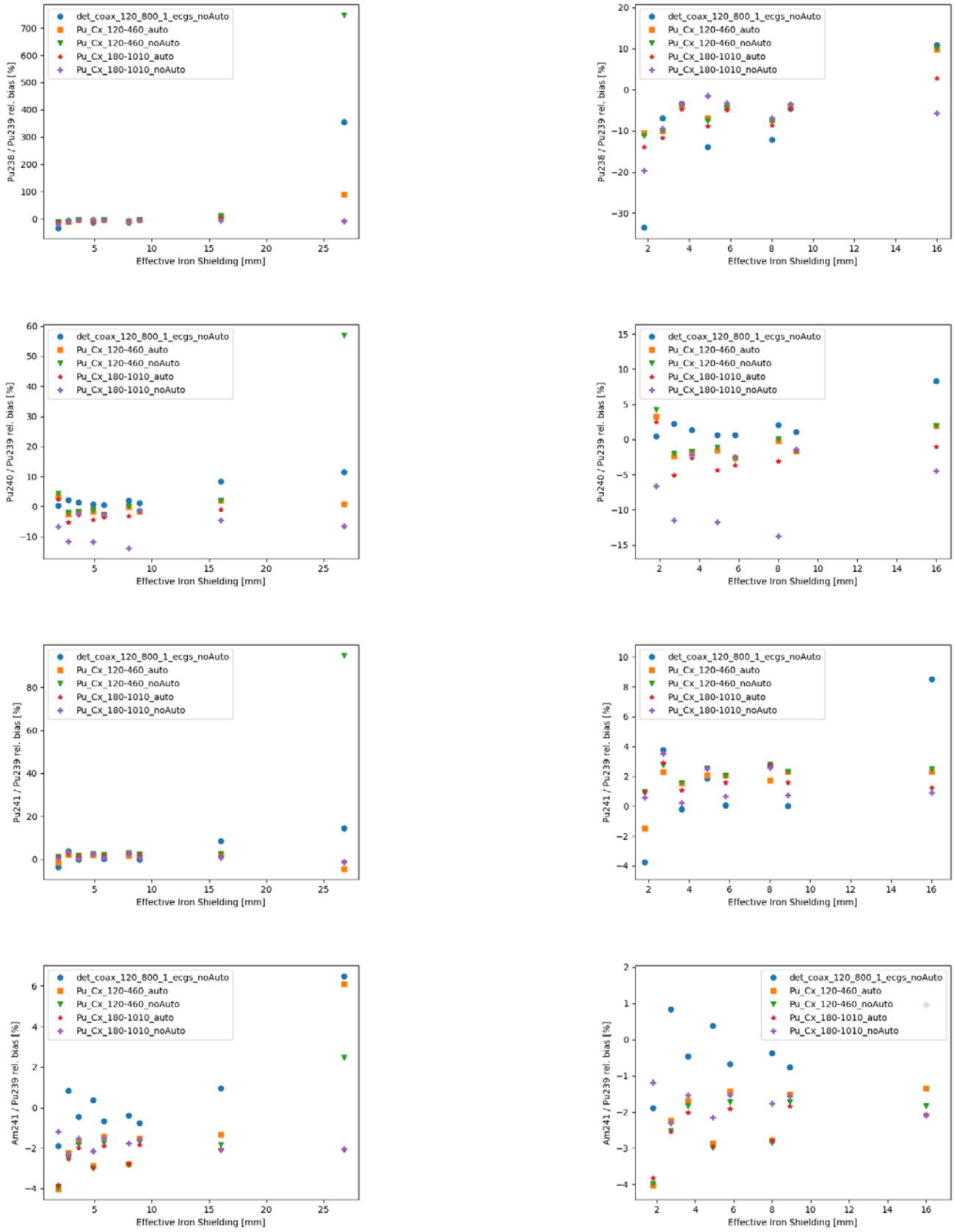

Figure 15: The average relative bias of the mass ratios as a function of effective iron shielding thickness: entire range (left) and zoomed-in to lower shielding values (right). Some points overlap, and that is why for some shieldings less than 5 points are visible. For example, Pu_Cx_180-1010 and Pu_Cx_180-1010_auto overlap for the highest shielding, because auto analysis always gives the final result using Pu_Cx_180-1010 in case of such thick shielding.

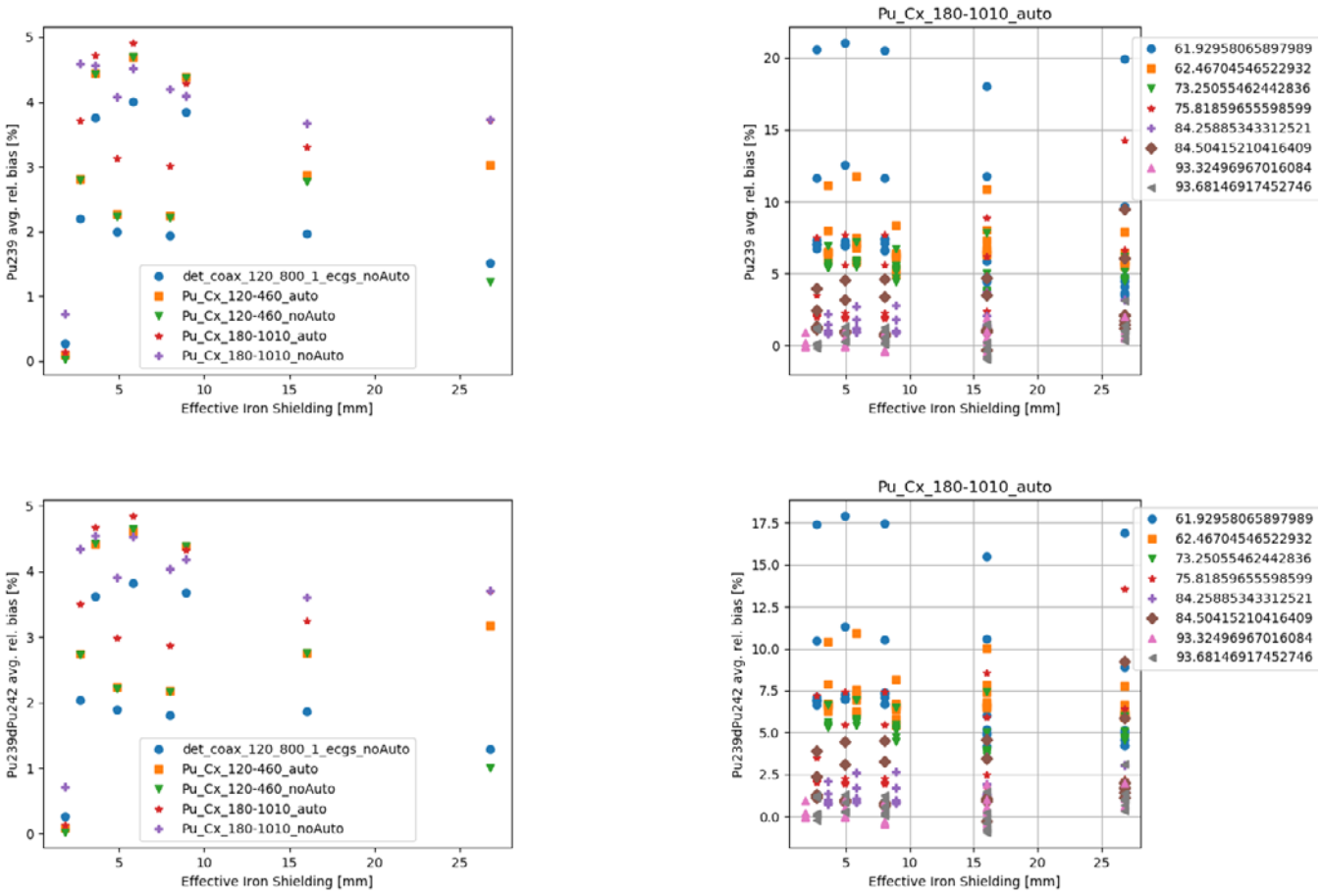

Figure 16: *Top left:* Average relative bias of the ^{239}Pu fraction as a function of effective iron shielding thickness for all parameter sets. *Top right:* Average relative bias of the ^{239}Pu fraction as a function of effective iron shielding, calculated using the parameter set Pu_Cx_180-1010 with auto analysis turned on, categorized according to the value of the declared ^{239}Pu. *Bottom left and bottom right*: the same as above, but using declared ^{242}Pu values.

3.4 When FRAM analysis fails

In some situations, especially for low quality spectra and for thick shielding, FRAM is not able to calculate one or more mass ratios and reports a zero for that mass ratio. The spectra for which FRAM gives a zero result were not included in the averages. Figure 17 shows the number of spectra for which a given parameter set failed to calculate a given mass ratio, that is, reported a zero result. Figure 18 shows the average number of zeros as a function of statistical quality.

From Figure 6 to Figure 16 one can see that for good quality spectra the best results for the various mass ratios are reported by the one of the two default parameter sets Pu_Cx_120-460 and Pu_Cx_180-1010 with auto analysis turned on. However, in case of low spectrum quality the default parameter sets often fail (i.e., report zero mass ratio) and in that case the parameter set det_coax_120_800_1_ecgs, which uses simultaneously the high and low energy region, provides the optimum results, as seen on Figure 17 and Figure 18.

As mentioned above, and as shown in Figure 18, FRAM failures happen with low quality spectra. Most FRAM failures happen with the 5 minute spectra and PIDIE samples as illustrated in Figure 19, showing, as an example, the average number of zeros for the ^{238}Pu/^{239}Pu ratio.

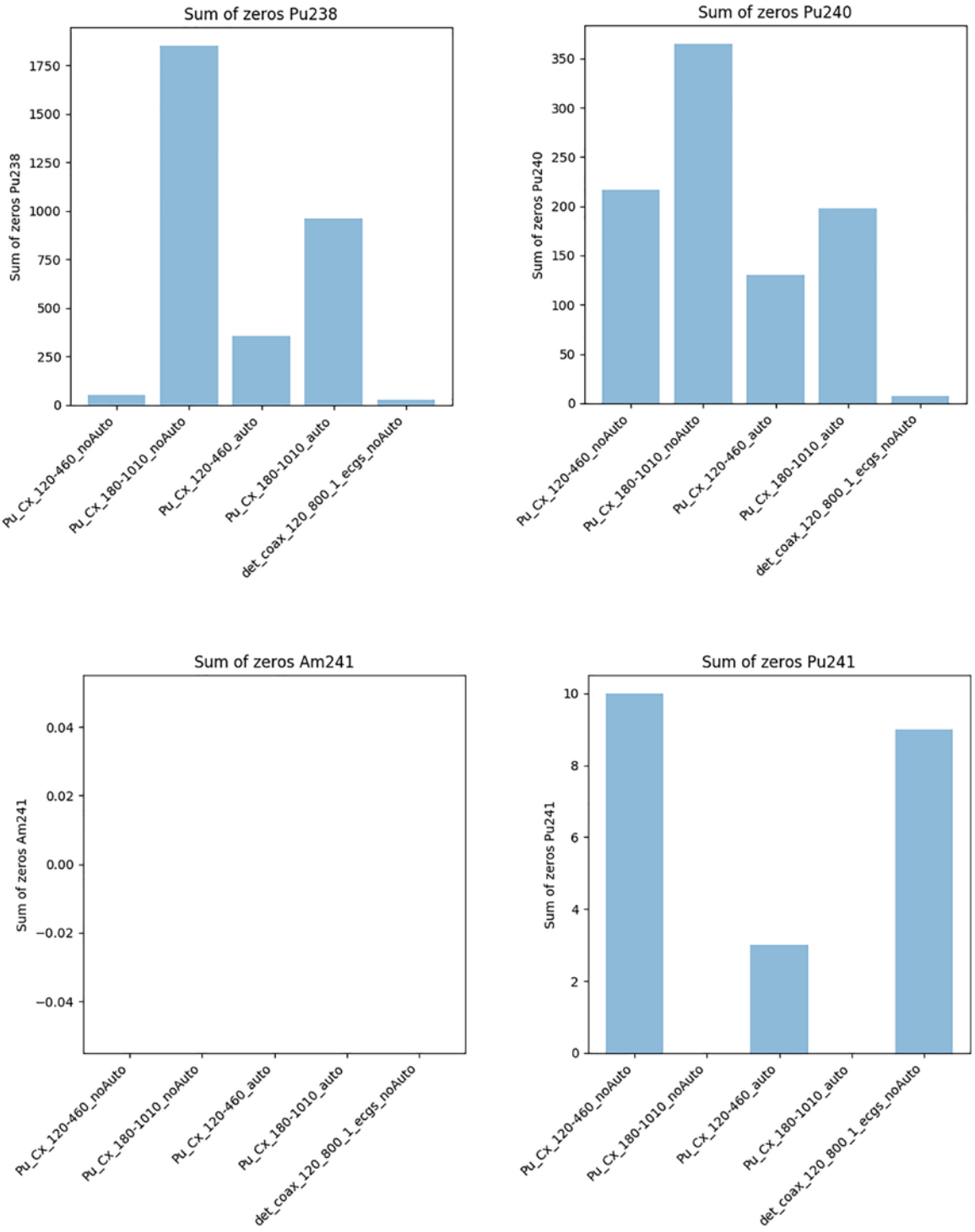

Figure 17: The sum of zeros (failures), out of 11240 analysed spectra, for the various mass ratios for different parameter sets. For ^{241}Am FRAM never fails with zero results.

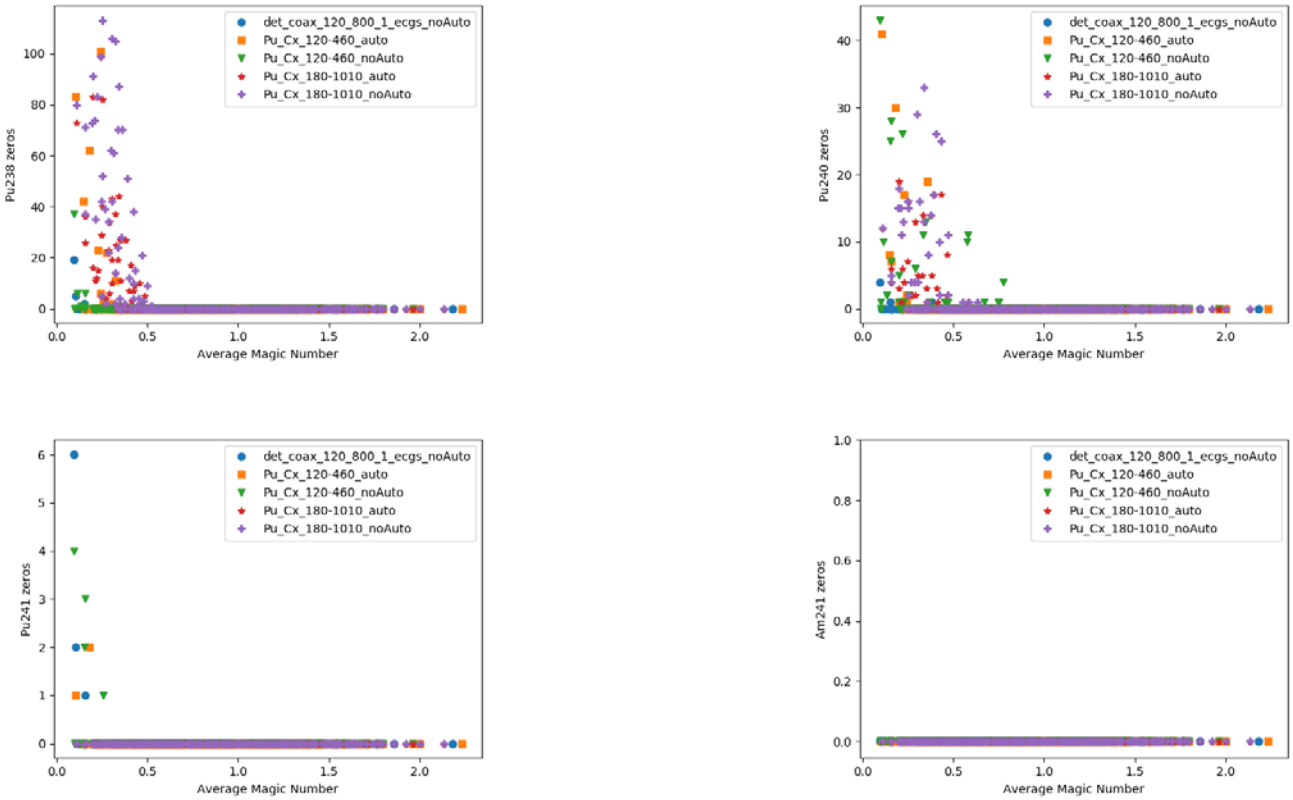

Figure 18: The average number of zeros of the various mass ratios as a function of statistical quality of the spectra, for all parameter sets

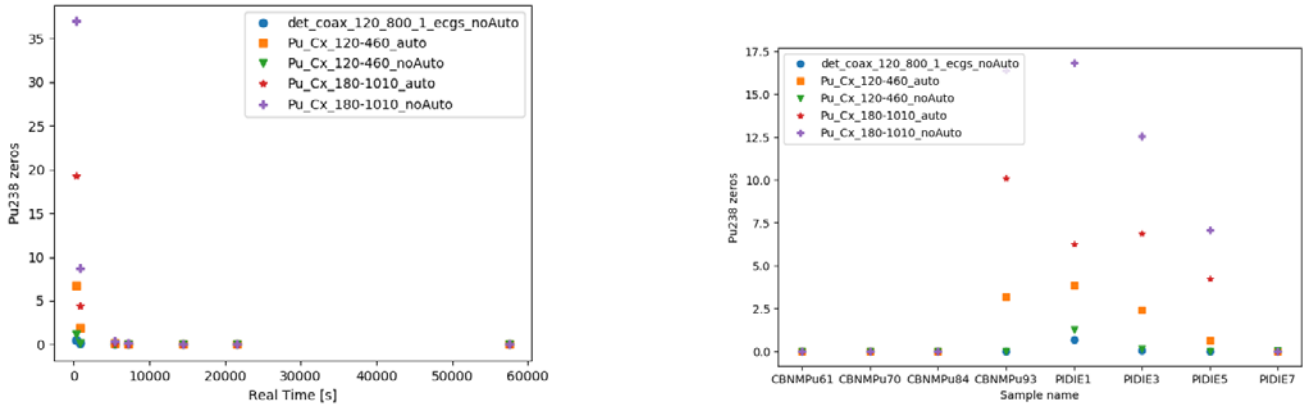

Figure 19: Average number of zeros for the $^{238}Pu/^{239}Pu$ ratio, as a function of real time (left) and sample name (right).

4. Conclusion

The auto analysis option significantly improves the performance of the default parameter sets Pu_Cx_120-460 and Pu_Cx_180-1010, especially in the case of lower quality spectra. This option enables FRAM to distinguish, e.g., shielded and unshielded samples and automatically re-analyse the spectrum using a parameter set that is better suited for the particular setup.

For the mass ratios relative to ^{239}Pu the default parameter sets (with auto analysis on) provide similar results, better than the set det_coax_120_800_1_ecgs. However, for the ^{239}Pu fraction the set det_coax_120_800_1_ecgs is superior to both default sets.

FRAM results heavily depend on the statistical quality of the spectra, as expected. A statistical indicator, called the "magic number", was used in this work to measure the statistical quality of the spectra. If this number is below 1, then the bias of the results can go up several orders of magnitude, especially for the ^{238}Pu/^{239}Pu mass ratio. For some of the measured samples the "magic number" does not go above 1, even for long measurement times and thin shielding, due to their low activity.

To improve the results for the ^{239}Pu fraction, it would be essential to improve the calculation of the ^{240}Pu/^{239}Pu ratio. Another step forward could be to create parameter sets accompanying the set det_coax_120_800_1_ecgs, in order to benefit from the possibilities offered by auto analysis.

These conclusions are valid for very old (>20 years), pure Pu samples. The extension of the studies to 1-2 years old MOX samples is planned.

5. References

[1] J. Zsigrai, A. Frigerio, J. Bagi, A. Mühleisen, and A. Berlizov, "Using FRAM to determine enrichment of shielded uranium by portable electrically cooled HPGe detectors," in *Proceeidings of the 39th ESARDA Annual Meeting - Symposium, 16-18 May 2017, Düsseldorf, Germany*, 2017, pp. 80–86.

[2] T. E. Sampson and T. A. Kelley, "PC/FRAM: A code for the non-destructive measurement of the isotopic composition of actinides for safeguards applications, LA-UR-96-3543," 1996.

[3] T. E. Sampson, T. A. Kelley, and D. T. Vo, "Application Guide to Gamma-Ray Isotopic Analysis Using the FRAM Software, LA-14018," 2003.

[4] D. T. Vo, "Operation and Performance of FRAM Version 5.1 Proceeding of the 52nd Annual Meeting of The Institute of Nuclear Materials Management, Palm Desert, CA, USA, July 17-21, 2011, LA-UR-11-03016," 2011.

[5] "Micro-Detective Ultra light, Portable Hand Held Radioisotope Identifier." https://www.ortec-online.com/products/nuclear-security-and-safeguards/hand-held-radioisotope-identifiers-riids/micro-detective (accessed Mar. 29, 2020).

[6] "CBNM Nuclear Reference Material 271, Certificate of Analysis, Commission of the European Communities, Joint Research Centre, Central Bureau for Nuclear Measurements, Geel," Geel, 1989.

[7] R.J.S. Harry, "PIDIE, plutonium isotopic determination inter-comparison exercise, ECN-RX--90-044," in *Annual Meeting of the Institute of Nuclear Materials Management*, 1990, no. July, pp. 15–18.

[8] J. Morel and B. Chauvenet, "Intercomparaison des mesures de composition isotopique du plutonium par spectrometrie X et gamma. Resultats de l'action 'Pidie', rapport final, CEA Centre d'Etudes de Saclay, Gif-sur-Yvette (France). Dept. des Applications et de la Metrologie des Rayonnem."

[9] J. Morel, B. Chauvenet, and M. Etcheverry, "Final results of the PIDIE intercomparison exercise for the plutonium isotopis determination by gamma spectrometry," in *Proceedings of the 13th ESARDA Symposium, Avignon, France*, 1991, pp. 251–257.

[10] C. T. Chantler *et al.*, "Detailed Tabulation of Atomic Form Factors, Photoelectric Absorption and Scattering Cross Section, and Mass Attenuation Coefficients for Z = 1-92 from E = 1-10 eV to E = 0.4-1.0 MeV," 2005. https://www.nist.gov/pml/x-ray-form-factor-attenuation-and-scattering-tables (accessed Aug. 01, 2018).